LABORATORY VERIFICATION OF BLAST-INDUCED LIQUEFACTION MECHANISM

Prepared for

USAF - OFFICE OF SCIENTIFIC RESEARCH
Bolling AFB
Washington, D.C.

Grant No. AFOSR-81-0085

By

Richard J. Fragaszy
Assistant Professor
and
Michael E. Voss
Research Assistant

Department of Civil Engineering
SAN DIEGO STATE UNIVERSITY
San Diego, California

October 1981

SDSU Civil Engineering Series No. 81145

UNCLASSIFIED

SECURITY CLASSIFICATION OF THIS PAGE (When Data Entered)

REPORT DOCUMENTATION PAGE		READ INSTRUCTIONS BEFORE COMPLETING FORM
1. REPORT NUMBER AFOSR-TR- 81 -0843	2. GOVT ACCESSION NO.	3. RECIPIENT'S CATALOG NUMBER
4. TITLE (and Subtitle) LABORATORY VERIFICATION OF BLAST-INDUCED LIQUEFACTION MECHANISM		5. TYPE OF REPORT & PERIOD COVERED FINAL Jan 81 - Jul 81 6. PERFORMING ORG. REPORT NUMBER
7. AUTHOR(s) RICHARD J FRAGASZY MICHAEL E VOSS		8. CONTRACT OR GRANT NUMBER(s) AFOSR [redacted] 81-0085
9. PERFORMING ORGANIZATION NAME AND ADDRESS SAN DIEGO STATE UNIVERSITY DEPARTMENT OF CIVIL ENGINEERING SAN DIEGO, CA 92182		10. PROGRAM ELEMENT, PROJECT, TASK AREA & WORK UNIT NUMBERS 61102F 2307/D9
11. CONTROLLING OFFICE NAME AND ADDRESS AIR FORCE OFFICE OF SCIENTIFIC RESEARCH/NA BOLLING AFB, DC 20332		12. REPORT DATE October 1981 13. NUMBER OF PAGES 52
14. MONITORING AGENCY NAME & ADDRESS(if different from Controlling Office)		15. SECURITY CLASS. (of this report) UNCLASSIFIED 15a. DECLASSIFICATION/DOWNGRADING SCHEDULE

16. DISTRIBUTION STATEMENT (of this Report)

Approved for public release; distribution unlimited.

17. DISTRIBUTION STATEMENT (of the abstract entered in Block 20, if different from Report)

18. SUPPLEMENTARY NOTES

19. KEY WORDS (Continue on reverse side if necessary and identify by block number)

BLAST-INDUCED LIQUEFACTION
CRATERING
SOIL MECHANICS
SOIL DYNAMICS
SAND
MATERIAL PROPERTIES
ENIWETOK SAND

20. ABSTRACT (Continue on reverse side if necessary and identify by block number)

A mechanism for blast-induced liquefaction was tested in a series of high pressure undrained, isotropic compression tests on saturated samples of Eniwetok beach sand and Ottawa sand. The theory, based on inelastic volume compressibility of sand, was shown to be valid for the case of quasi-static, isotropic loading. Specimens of Eniwetok sand subjected to an initial effective stress of 1 MPa were liquefied by a single cycle of loading of 34 MPa. Specimens of Ottawa sand, tested in the same manner, generated excess pore

DD FORM 1 JAN 73 1473 EDITION OF 1 NOV 65 IS OBSOLETE

UNCLASSIFIED 4/2 7/6 cont K

SECURITY CLASSIFICATION OF THIS PAGE (When Data Entered)

pressure but not enough to completely liquefy the soil. The errors introduced by flexibility of the testing system were analyzed and found to be insignificant. Suggestions for future research were made.

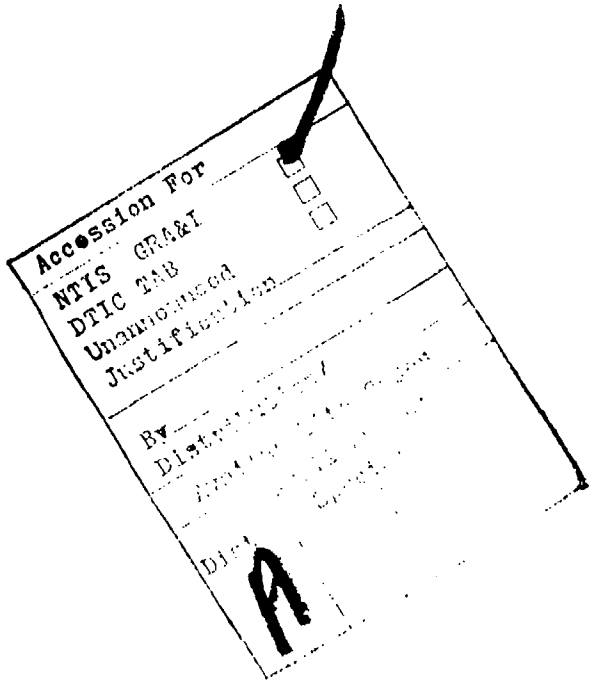

(13)

Conditions of Reproduction

Reproduction, translation, publication, use and disposal in whole or in part by or for the United States Government is permitted.

[illegible] (AFSC)
[illegible] is
Distribution [illegible] AFR 190-12.
MATTHEW J. KETTER
Chief, Technical Information Division

TABLE OF CONTENTS

LIST OF FIGURES

LIST OF TABLES

SECTION I

INTRODUCTION

1.1 BACKGROUND

The effects of nuclear weapons on geologic materials at and near the ground surface are an important concern of the Air Force. The volume and shape of craters and the intensity, duration and extent of ground shock are all influenced by local soil conditions. In recent years, there has been an increasing interest in the phenomenon known as blast-induced liquefaction. In this context, the term "liquefaction" has been defined by the American Society of Civil Engineers as "the act or process of transforming any substance into a liquid. In cohesionless soils, the transformation is from a solid state to a liquid state as a consequence of increased pore pressure and reduced effective stress" (1). In recent reviews, Melzer (2) and Blouin (3) have discussed the occurrence of blast-induced liquefaction in several high-energy field tests (PRAIRIE FLAT; DIAL PACK; Pre-DICE THROW II, SNOWBALL). Surface water spouts, sand boils, material subsidence and flow are some of the indications that liquefaction was caused by these explosions. Also of significance are the unusually broad and flat craters produced by the Pre-DICE THROW II and SNOWBALL events. These craters are similar in shape to those produced at the Pacific Testing Grounds. This lends support to the hypothesis that the unique shape of the Pacific craters may have been caused by

massive liquefaction flow slides into a transient bowl shaped crater.

Liquefaction can also be produced by earthquake-induced shear stresses. In fact, the phenomenon of earthquake-induced liquefaction has been studied intensively for almost two decades, and the mechanism causing it is fairly well understood. Tests have been developed to determine the liquefaction susceptibility of soils, and methods to predict the occurrence of liquefaction are growing steadily more sophisticated. In contrast, very little work has been done on blast-induced liquefaction. While theories have been proposed to explain the phenomenon, none have been conclusively verified. At this time, there is no accepted method available to evaluate the susceptibility of a specific site to blast-induced liquefaction or to determine the effects of liquefaction on crater geometry, hardened structures, etc., if it does occur. To begin to answer these questions, it is important that the basic mechanism be determined. The major objective of this study was directed to this end.

1.2 OBJECTIVE AND SCOPE

The ultimate objective of this line of research is to verify and quantify the mechanism causing blast-induced liquefaction, and to use this information to predict the occurrence and effects of blast-induced liquefaction. This report describes the initial efforts toward this goal. The objective of this specific project is to verify the blast-induced liquefaction mechanism proposed by Prater (4) and Rischbieter et al (5). The scope is limited to quasi-static tests in which the fundamental aspects of the theory are tested.

SECTION II

THEORY

2.1 DESCRIPTION OF PROPOSED MECHANISM

Prater (4) and Rischbieter et al (5) have proposed a theory to explain the blast-induced liquefaction mechanism. In their model the initial compression wave from an explosion passes through the soil, compressing both the soil matrix and the pore water. If the soil is fully saturated, the increase in effective stress will be only a very small fraction of the increase in pore water pressure. This is due to the large bulk modulus of water compared to a typical bulk modulus of a granular soil. The relationship between the rise in pore water pressure (Δu) and the isotropic stress increase ($\Delta\sigma_3$) is usually expressed by the following equation developed by Skempton (6):

$$\Delta u = B\Delta\sigma_3 \quad \ldots\ldots\ldots\ldots\ldots\ldots\ldots\ldots\ldots\ldots \quad (1)$$

where B is referred to as the pore pressure parameter.

For a saturated soil under perfectly undrained conditions, B can be calculated from the compressibility of water, c_w, and the compressibility of the soil skeleton, m_v, as follows (7):

$$B = \frac{1}{1 + n\,(c_w/m_v)} \quad \ldots\ldots\ldots\ldots\ldots\ldots\ldots\ldots \quad (2)$$

where n is the porosity of the soil. Typical values of m_v range between 2×10^{-3} m^2/KN for a very soft clay to 5×10^{-6} m^2/KN for a moderately dense sand. Using these two values and the compressibility of water (approximately 4.67×10^{-7} m^2/KN), the value of B ranges between 0.9999 for soft clay to 0.9538 for dense sand.

In normal soil mechanics practice the effective stress increase would be neglected. When the total stress increase is large, however, it must be considered. The changes in effective stress and pore water pressure caused by a passing compression wave are shown in Figure 1. The initial state of effective stress in the soil is represented by point B and the initial pore pressure by point A. The path BD represents the change in effective stress due to a passing compression wave. The pore water pressure increases also, as shown by path AC. As the compression wave passes, the pore water phase unloads elastically along path CA; however, the soil matrix is assumed to unload inelastically along path DE, just as it would if there were no water present or if the loading were completely drained. Because of the large hysteresis in the stress-strain path for the soil matrix, it is possible that the effective stress could drop to zero when the pore pressure is at some positive value, F. This condition meets the definition of liquefaction--zero effective stress. Whether or not a given volume of soil will liquefy will depend on the initial state of stress in the soil, the magnitude of the compression wave, the relative compressibility of the soil matrix and pore water, and the stress-volumetric strain relationship for the soil.

Two major assumptions are made in this theory. The first is that the dynamic strain is the same in the soil matrix and the pore

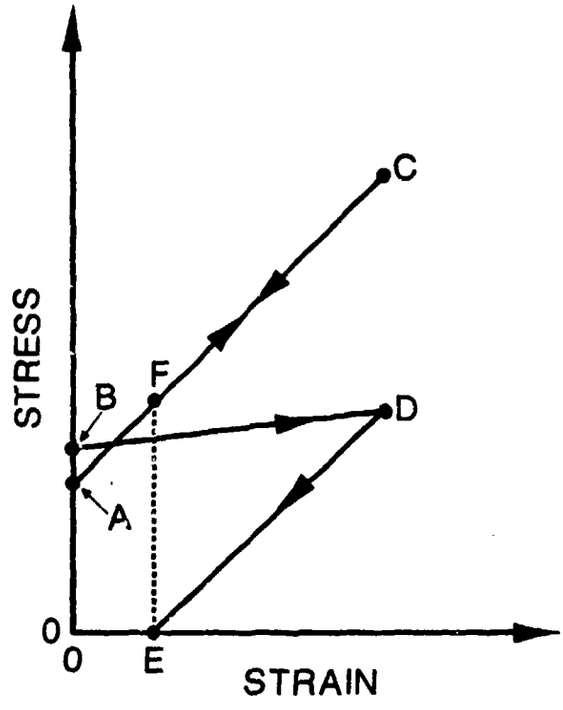

Fig. 1 Model for Blast-Induced Liquefaction

water. This is possible only if there is no separation of the wave fronts in the soil matrix and the water. This assumption has been verified for blast-induced waves both mathematically by Ishihara (8) and experimentally by Rischbieter et al (5) and Lyakhov and Polyyakova (9). The second assumption is that the hysteresis observed in the stress-strain curve during drained loading is also present during undrained conditions. This assumption has not been proven and, in fact, Cristescu (10) states that a saturated soil behaves elastically and therefore undergoes no permanent volume change. If this is true, the proposed mechanism is not possible.

2.2 PREVIOUS LABORATORY AND FIELD WORK

The laboratory and field experiments performed to date have supported the proposed liquefaction mechanism but have neither conclusively proven its validity nor provided the data needed to predict large scale behavior. Kok (11) has caused liquefaction to occur in a laboratory experiment in which a plexiglass permeameter was filled with sand and saturated with deaired water. The cylinder was then struck by a pendulum and both change in void ratio and pore water pressure were recorded. Kok (11) also conducted small scale field experiments with up to 100 Kg of TNT. These field tests indicate that the horizontal zone of liquefaction increases as the cube root of the charge weight. Both these experiments, however, were concerned with the compaction of soil. No data on the magnitude of the stress waves were obtained.

Studer and Hunziker (12) have conducted shock tube experiments in which liquefaction was observed. They were unable, however, to

produce 100% saturation in their test apparatus. Rischbieter et al also were unable to obtain 100% saturation in their field tests. This is very important because the compressibility of water is greatly increased by even a very small amount of undissolved air. For example, a change in the degree of saturation from 100% to 99.9% increases compressibility from 4.67×10^{-7} m^2/KN to 7.44×10^{-6} m^2/KN (13), resulting in a drop in B value to approximately 0.6 for a moderately dense sand.

As the compressibility of the pore water increases, it becomes more difficult to achieve liquefaction. Since natural soils below the permanent water table are saturated, it is important to conduct liquefaction experiments with completely saturated soils; otherwise, liquefaction potential will be underestimated. Rischbieter (14) cites the difficulty in obtaining complete saturation as one of the major problems in performing blast-induced liquefaction studies. In the experiments described below, particular attention was paid to the problem of sample saturation.

SECTION III

EXPERIMENTAL WORK

3.1 INTRODUCTION

The principal objective of this project is to determine if the blast-induced liquefaction mechanism proposed by Prater (4) and Rischbieter et al (5) can be verified in a reasonably simple laboratory experiment. Rather than attempt to design and carry out a complicated and expensive dynamic experiment in which all components of the problem are simulated, it was decided that the central assumption of the theory should be tested first. An experiment was designed to test whether or not a saturated granular soil would behave elastically under a single cycle of compressive load. The simplest type of loading, isotropic, was chosen because of the ease with which it could be produced. It was felt that if the soil behaves inelastically under isotropic loading conditions, certainly an anisotropic loading would also produce inelastic behavior.

3.2 EXPERIMENTAL DESIGN

To test the proposed mechanism in the manner described above, an experiment which meets the following criteria is required. First, a method of sample preparation must be used which minimizes variation in density and structure between tests. Second, 100% saturation must

be achieved in a reasonable length of time without using excessively high backpressure. Third, deviations from totally undrained conditions must be minimized. Fourth, the total, effective and pore water pressures must be accurately recorded.

Because these criteria have been met by earthquake liquefaction researchers using triaxial testing equipment, it was decided to use similar equipment for the blast-induced liquefaction experiments. A high pressure triaxial system, described in the following section, was modified for these experiments. The choice of a triaxial testing system dictated the use of a cylindrical test specimen. Using the standard procedures for preparation of a cohesionless test specimen, variation between samples is minimal.

To saturate the test specimens, the CO_2 method of saturation, first described by Lade and Duncan (15) was used. This requires flushing the dry sand specimen with CO_2 gas as the specimen is being formed. Next, a vacuum is applied to the specimen to remove as much CO_2 gas from the voids as possible. Deaired water is then introduced into the sample and a backpressure is applied. This procedure produces a high initial degree of saturation which increases to 100% as the CO_2 bubbles dissolve in the water. The length of time required to saturate the soil is a function of the initial degree of saturation, the back pressure and the solubility of the gas in the voids of the soil. The reason for flushing the sample with CO_2 is apparent when the work by Black and Lee (16) is reviewed. They determined the time to saturate a sand with a similar procedure but without CO_2 flushing. Even with a high initial degree of saturation and backpressure, a week or more was required. Since CO_2 has a solubility

in water almost two orders of magnitude greater than air, saturation can be accomplished in less than one day at significantly lower back-pressures than required when the voids are initially filled with air.

After the specimen is saturated, the initial total stress (cell pressure) and pore water pressure are established. To produce the required cycle of isotropic loading the cell pressure is increased to a predetermined level, then returned to its initial value. The cell pressure and pore water pressure are monitored with pressure transducers located just outside the triaxial cell. During the loading cycle the drainage line out of the specimen is closed beyond the transducer. The very short length of tubing from the specimen to the transducer and the stiffness of the tubing and the transducer diaphragm minimize the volume of water which flows out of the soil as the pore pressure rises. Also, the use of brass shim stock between the soil and the triaxial membrane reduces the effects of membrane penetration into the voids of the soil. The effects of these deviations from truly undrained conditions are discussed in more detail in Section V.

If the proposed theory is correct, the pore water pressure at the end of the load cycle should be higher than at the beginning. If liquefaction occurs the effective stress will be zero and, therefore, the pore water pressure will equal the cell pressure.

3.3 EQUIPMENT

The equipment used for the isotropic compression test centered around a 70 MPa working pressure steel triaxial cell which uses a Wykeham Farrance 70 MPa constant pressure pump to provide the rapeseed

oil confining fluid at the desired pressure. The cell and pump are shown in Figs. 2 and 3, respectively. The cell pressure was monitored by a Senso-Metrics, Inc. pressure transducer. The soil sample used in these tests measures approximately 3.5 cm in diameter and 10.5 cm in height. Fig. 4 shows the sample in place in the triaxial cell. A schematic drawing of the assembled test specimen is shown in Figure 5. The bottom pedestal contains a drainage line so that fluid can enter or leave the sample as necessary. A porous brass cap is located between the sample and the bottom pedestal to prevent soil from entering the drainage line. The top loading cap is solid steel without any drainage line. The loading piston fits into the top cap and is used in a standard triaxial test to apply the axial deviator stress to the sample. The sample is confined by a 7.6 mm thick rubber triaxial membrane sealed at the top and bottom with 4 O-rings. Between the sample and the triaxial membrane are two sheets of 0.05 mm thick shim brass, 5.3 cm by 10.2 cm. These sheets were placed lengthwise inside the membranes with a small gap between the brass and the top and bottom caps to allow free isotropic compression. The equipment used to saturate the sample and monitor the pore pressure is shown schematically in Fig. 6. The main components of this system include a second pressure transducer to measure pore pressure, a carbon dioxide tank, a pressurized deaired water supply and a vacuum pump.

Both of the pressure transducers are connected to an X-Y recorder so that plots of pore pressure vs. confining pressure can be made during the test as shown in Fig. 7. Because the effective stress is the total stress (cell pressure) minus the water pressure, it can easily be determined by measuring the distance to a 45° line drawn

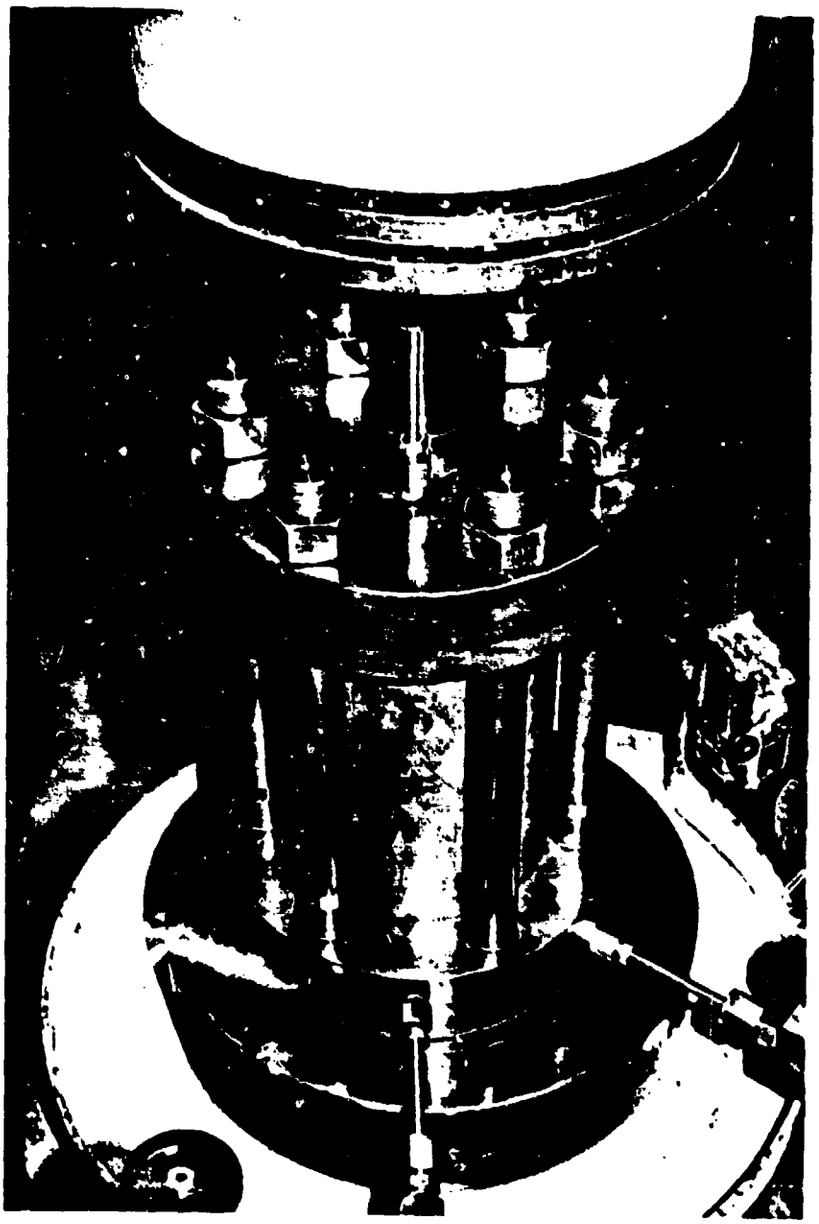

Fig. 2 High Pressure Triaxial Cell

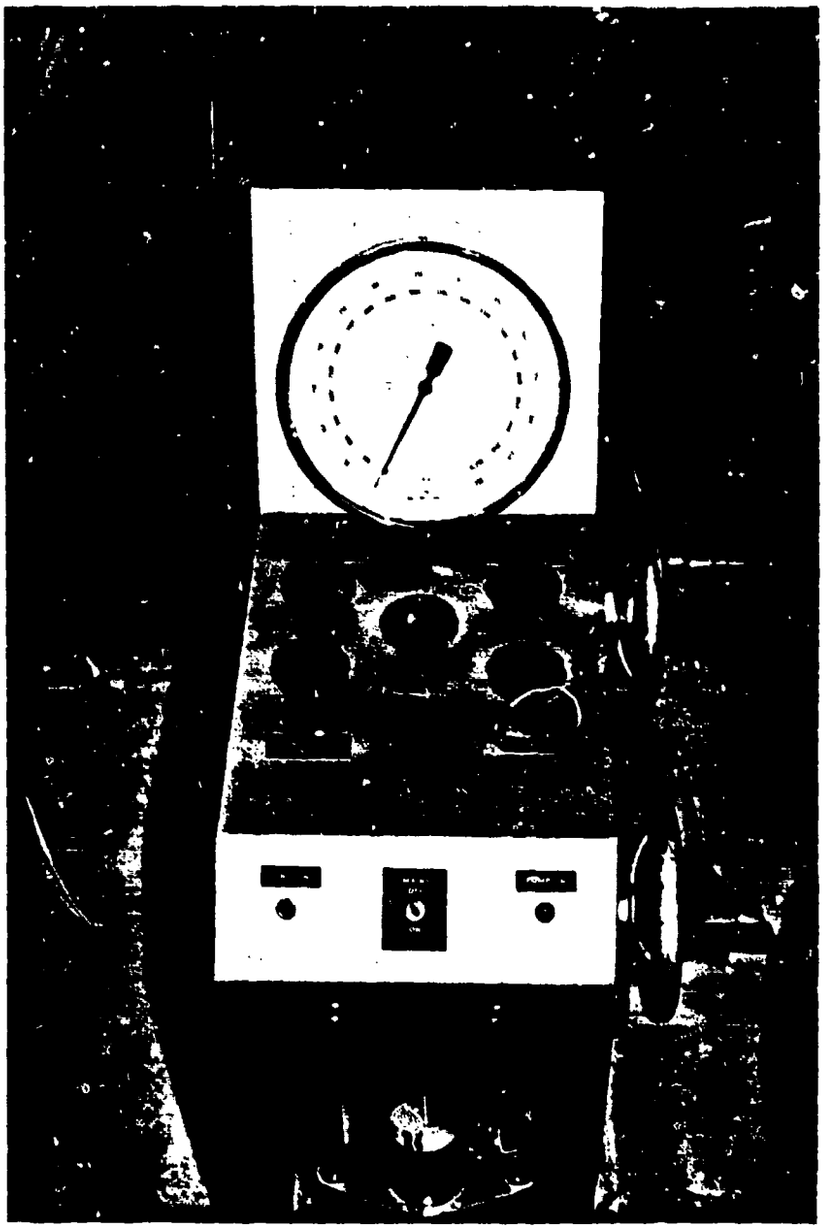

Fig. 3 70 MPa Pump for Triaxial Cell

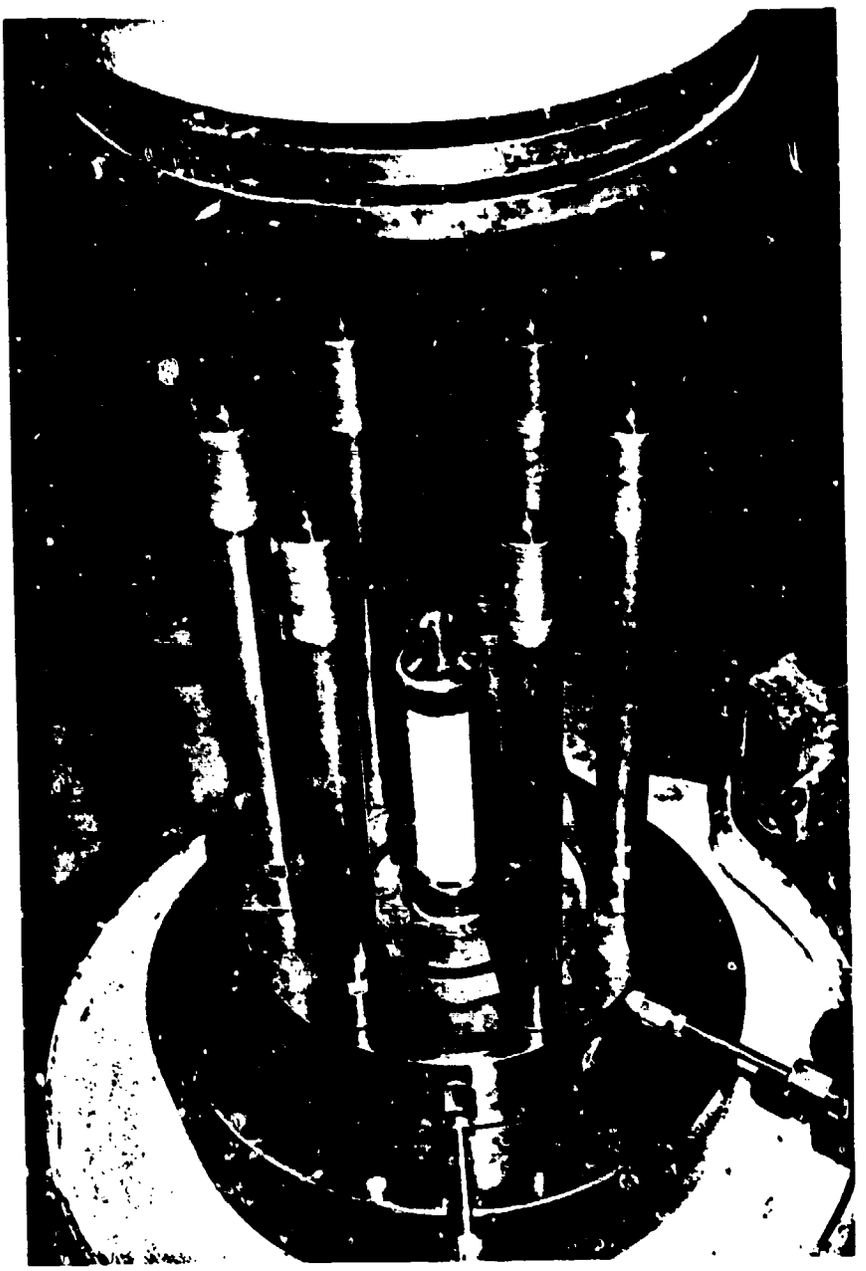

Fig. 4 Assembled Test Specimen

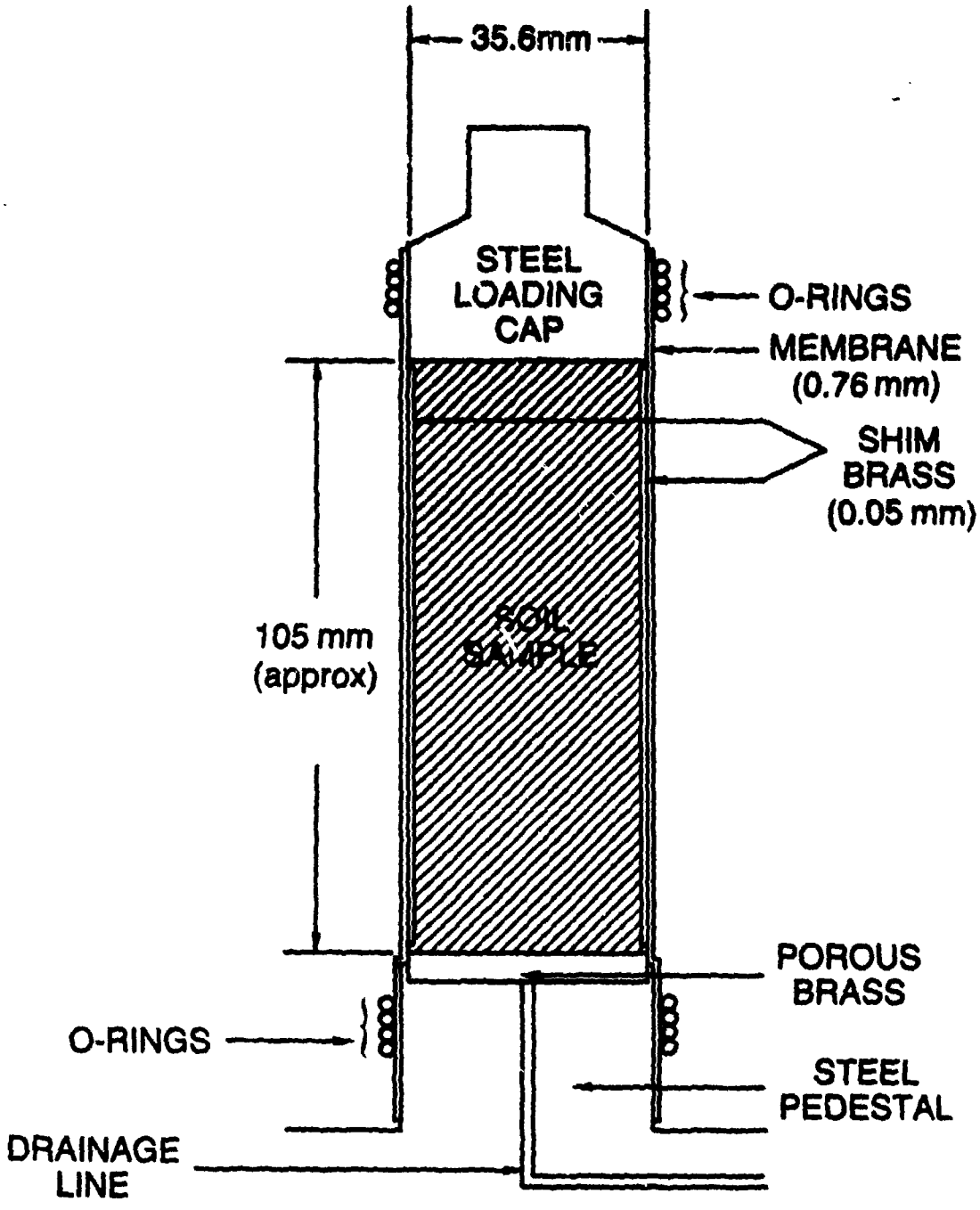

Fig. 5 Schematic Diagram of Assembled Test Specimen

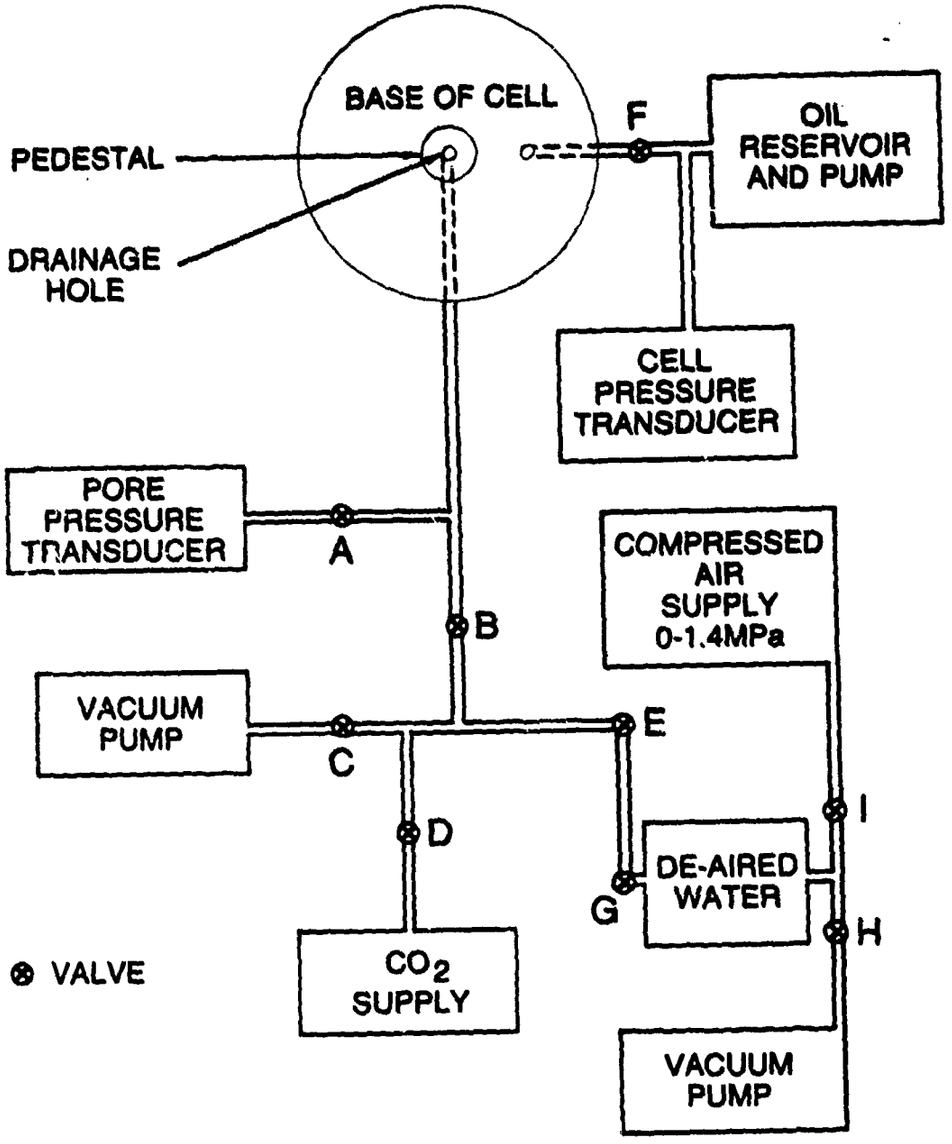

Fig. 6 Schematic Diagram of Plumbing System

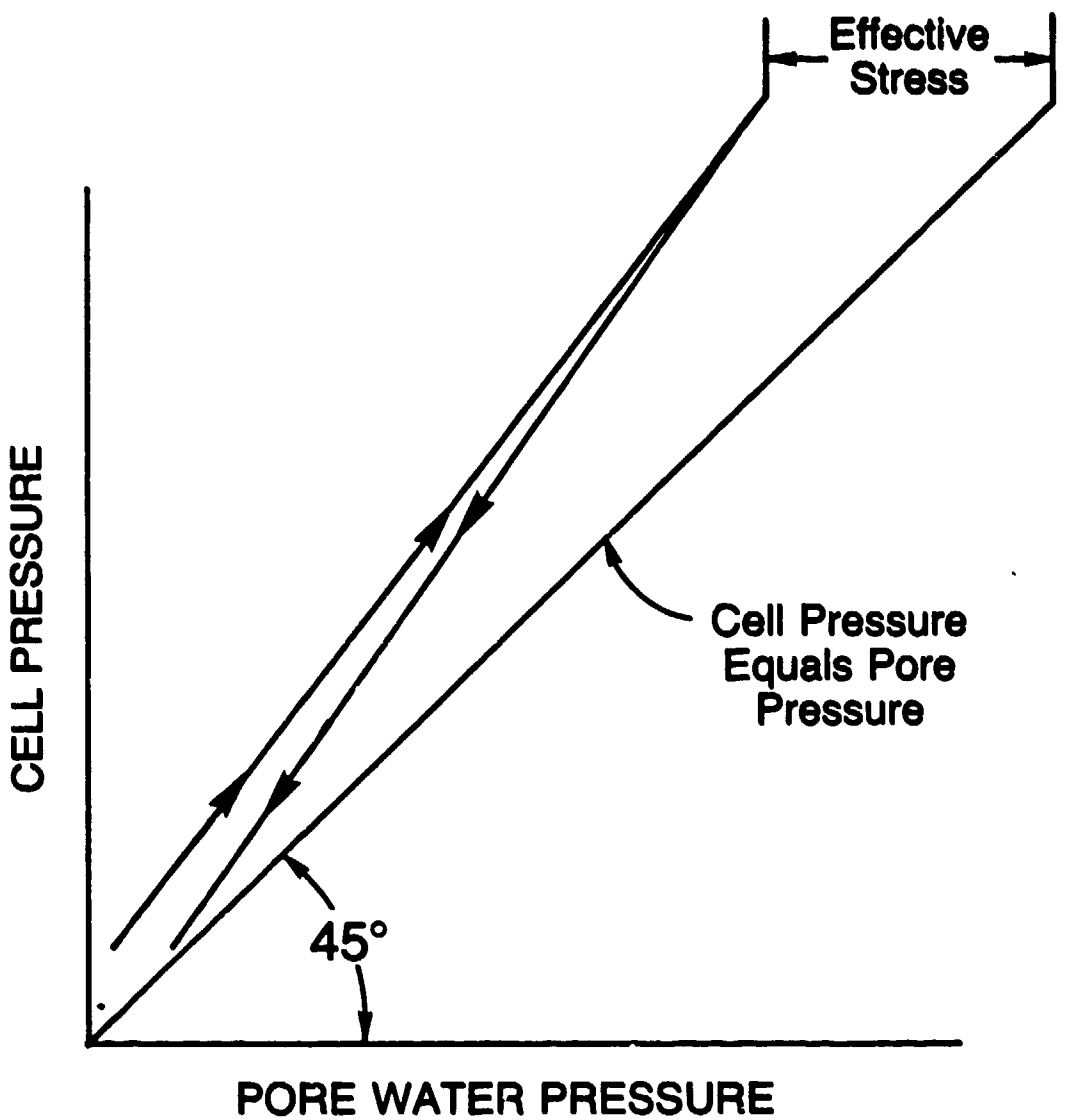

Fig. 7 Typical Form of X-Y Recorder Data

through the origin. It should be pointed out that the location of both pressure transducers preclude any accurate measurements of dynamic pressure events. At the loading rate for these tests, however, the problems associated with the locations of these transducers are minimal.

All tubing and valves between the cell and valve B, including valve B, are stainless steel with a minimum allowable working stress in excess of 70 MPa. The remainder of the system is not subjected to high pressures and lower strength valves, and lower strength valves and tubing are used. A photograph of this portion of the plumbing system is shown in Fig. 8.

3.4 SOIL DESCRIPTION

Several soils were used in these experiments in an attempt to determine the range of behavior possible. Most tests were performed on Eniwetok beach sand. Also used were three types of Ottawa sand known as Flintshot, Banding and Sawing sand. A summary of density and grading information for these sands is given in Table 1. More detailed information on Eniwetok beach sand can be found in a report by Windham (17).

3.5 TEST PROCEDURE

The first step in the test procedure is to fill the line between valves E and G and from valve A to the pore pressure transducer with deaired water and to fill the line from the oil pump to the cell pressure transducer with oil. The next step is to form the sample. The soil to be tested is first oven dried and allowed to cool. This is done so that the exact dry weight of dry soil in the sample can

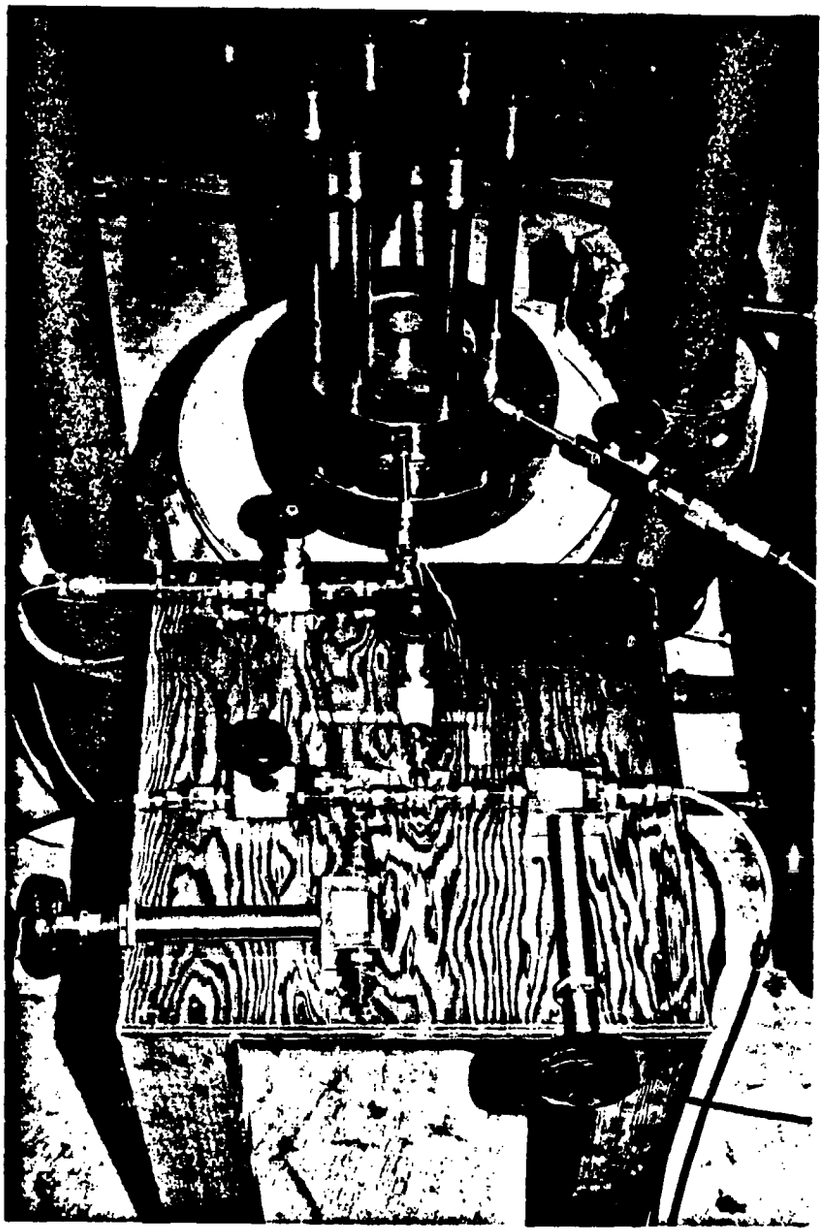

Fig. 8 Photograph of Valves and Tubing Used in Plumbing System

TABLE 1

Soil Properties

Sand	Minimum Dry Density (g/cm^3)	Mean Grain Size (mm)	Coefficient of Uniformity	Specific Gravity
Eniwetok	1.31	0.35	1.6	2.71
Ottawa (Flintshot)	1.57	0.60	1.4	2.66
Ottawa (Sawing)	1.56	0.50	1.3	2.66
Ottawa (Banding)	1.47	0.25	2.0	2.66

be measured. Next, the triaxial membrane is placed in the membrane mold. A partial vacuum (about 120 mm of mercury) is then pulled between the membrane and the mold to hold the membrane tightly against the mold. Next, the two sheets of .05 mm brass shim stock are placed inside the membrane and held in place with double stick tape. This is done to reduce the effects of membrane penetration. A small horizontal gap is left between the two sheets of brass to allow free isotropic compression.

To begin forming the sample the mold is placed over the triaxial cell pedestal. All valves are closed except B and D. The carbon dioxide tank is then opened and the gas allowed to flow through the tubing into the triaxial cell through the drainage line in the bottom pedestal. The soil is then carefully poured into the membrane. The resulting sample is quite loose due to the carbon dioxide bubbling up through it; the sample can be compacted to a denser state if desired. Once the membrane is filled, the steel loading cap, coated with silicon grease, is placed on top of the sample. The top of the membrane is pulled up over the cap, and the bottom of the membrane is pulled down over the greased pedestal. Next, the vacuum pump is started, valve D is closed, and then valve C is opened. This produces a vacuum of approximately 700 mm of mercury in the sample and in all the lines between valves A, C, D, and E. The vacuum in the sample produces a total confining pressure of about 100 KPa, permitting removal of the mold. O-rings are then placed over the membrane to seal the top and bottom of the sample. The height of the sample is now measured so that the density can be calculated. The second step in the test procedure is assembling the cell, opening valve F, and filling the cell with oil. This was a straightforward process.

Once the cell is filled with oil the pressurization and saturation process can begin. First, the cell pressure is raised to 690 KPa. Next, valve C is closed. At this time a vacuum still exists in the sample and all the lines bounded by valves A, C, D and E. Next, valve I is opened and a pressure of about 15 KPa is put on the deaired water tank. Valve B is then closed, valve G opened, then valve E is opened. Deaired water will begin to flow into the lines bounded by valves C, B, D and the deaired water supply. Now valve B is opened slowly, allowing deaired water to flow into the sample. Valve A is then opened, allowing measurement of pore water pressure. At this point in the test all the lines from valves C, D and E to the pore pressure transducer are filled with deaired water. The sample is now almost, but not quite, saturated, since the vacuum pump could not remove all the air and carbon dioxide in the system. The remaining gas must be dissolved in the water. As discussed above, the advantage of using carbon dioxide is that it takes much less time and lower pressures to dissolve it in water compared to air, and a larger volume of carbon dioxide can be dissolved at a given pressure.

After water no longer flows into the sample the water pressure (backpressure) is slowly increased to 690 KPa, while the cell pressure is simultaneously increased at the same rate to approximately 1.39 MPa. At no time is the effective stress higher than 700 KPa. When these stresses are reached the soil is subjected to an effective stress of 700 KPa. This state of stress remains on the sample overnight to provide ample time for the carbon dioxide to dissolve. The following day the cell pressure is increased to 1.72 MPa, while the backpressure remains at 0.7 MPa. While these initial stresses are to some extent

arbitrary, they do represent a reasonable ratio of total stress to pore water pressure. After allowing the sample to reach equilibrium under the new state of effective stress (about 1.03 MPa), valve B is closed, thus preventing drainage. Cell pressure is then increased until it reaches 34.5 MPa. The X-Y recorder clearly shows the small increase in effective stress due to this increased cell pressure. Cell pressure is then lowered until the initial 1.72 MPa is reached. As the unloading progresses the X-Y recorder will plot a line below the loading line if inelastic deformation occurs. If the soil behaves elastically, the loading and unloading lines will be the same. At the end of the unload cycle any difference between initial and final water pressure is a measure of the plastic volume change in the sample. Prater's theory predicts that if high enough stresses are reached this difference or "residual" water pressure will be sufficient to cause liquefaction. When this occurs, the unloading line will intersect the 45° line and follow it down until unloading is complete. The unloading line cannot cross below the 45° line because this would mean the pore water pressure is higher than the total confining pressure (cell pressure). Equilibrium would then require that the effective stress be negative, an impossible condition in a cohesionless soil.

SECTION IV

TEST RESULTS

4.1 INTRODUCTION

The initial test on each of the soils was conducted in the manner described above, with the exception that brass shim stock was not placed between the sample and the triaxial membrane. The results of these tests, shown in Table 2, were initially disappointing, since even the largest residual pore pressure generated was not nearly enough to cause liquefaction. For the Ottawa sands the residual pore pressure was negligible. The major reason for the problem has been identified in the literature on earthquake-induced liquefaction--a phenomenon known as membrane penetration (7, 18, 19, 20). In the initial part of the test the membrane is held tightly against the sand particles and actually penetrates into the voids of the sand. If the effective stress is lowered, as is necessary to produce liquefaction, the membrane will move out from the voids. This causes an increase in volume of the sample and prevents buildup of excess pore pressure. The solution to this problem is to add the brass shim stock between the soil and the triaxial membrane to minimize the penetration of the membrane into the soil. A detailed analysis of the effects of membrane penetration will be presented in the Discussion section. The remainder of this section will be devoted to a description of the results from those tests in which the brass was used.

TABLE 2

Results of Tests Conducted Without Brass Shim Stock

Soil	Dry Density (g/cc)	Test	Initial		Peak		End		Residual Water Pressure (MPa)
			Confining Pressure (σ_3, MPa)	Water Pressure (u, MPa)	Confining Pressure (σ_3, MPa)	Water Pressure (u, MPa)	Confining Pressure (σ_3, MPa)	Water Pressure (u, MPa)	
Eniwetok Beach Sand	1.39	E-2	1.72	0.69	34.5	32.4	1.72	1.17	0.48
Eniwetok Beach Sand	1.37	E-4	1.72	0.69	34.5	32.7	1.72	1.38	0.69
Eniwetok Beach Sand	1.38	E-5*	1.72	0.69	34.5	32.9	1.72	1.38	0.69
Ottawa Flintshot Sand	1.60	F-2	1.72	0.69	34.5	31.7	1.72	0.69	0

*E-5 - 72 hour saturation

4.2 TESTS ON ENIWETOK SAND

Nine tests were conducted using Eniwetok sand. These tests covered a range of dry densities from 1.30 to 1.45 gm/cm , and all resulted in liquefaction occurring during unloading. The results of these tests are shown in Table 3. Figures 9-12 present the data from four typical tests. In each of these tests the increase in effective stress is approximately the same, and liquefaction occurred at approximately the same cell pressure during unloading.

Test E-7 differed from the others in that after the first cycle of load (from 1.7 MPa to 34.5 MPa), the drainage line was opened to the pressurized water reservoir, allowing water to flow out of the sample. In this way the initial stress conditions were reestablished. The sample, of course, was denser due to the plastic volume change of the soil skeleton. A second test was then conducted, but with a cycle to only 6.9 MPa. This resulted in a residual pore pressure of 350 KPa, only one-third of the amount required to cause liquefaction. The initial stress conditions were then reimposed and a cycle of loading to 13.8 MPa was applied, causing a residual pore pressure of 700 KPa. In a like manner, additional cycles to 20.7, 27.6 and 34.5 MPa were applied. The cycle to 20.7 MPa caused a residual pore pressure of 860 KPa. The last two cycles caused liquefaction.

4.3 TESTS ON OTTAWA SAND

Tests were performed on three types of Ottawa sand: Flintshot, Sawing and Banding. The three sands differ only in grain size distribution. Flintshot is the coarsest, with a mean grain size of 0.60 mm. The Sawing and Banding sands have mean grain sizes of 0.50 and 0.25 mm,

TABLE 3

Results of Tests on Eniwetok Sand Conducted With Brass Shim Stock

Soil	Dry Density (g/cc)	Test	Initial		Peak		End		
			Confining Pressure (σ_3, MPa)	Water Pressure (u, MPa)	Confining Pressure (σ_3, MPa)	Water Pressure (u, MPa)	Confining Pressure (σ_3, MPa)	Water Pressure (u, MPa)	Residual Water Pressure (MPa)
Eniwetok Beach Sand	1.35	E-6	1.72	0.69	34.5	33.1	1.72	1.72	1.03
Eniwetok Beach Sand	1.31	E-7	1.72	0.69	34.5	33.1	1.72	1.72	1.03
		"	1.72	0.69	6.9	5.69	1.72	1.03	0.35
		"	1.72	0.69	13.8	11.7	1.72	1.38	0.70
		"	1.72	0.69	20.7	18.4	1.72	1.55	0.86
		"	1.72	0.69	27.6	25.5	1.72	1.72	1.03
		"	1.72	0.69	34.5	31.9	1.72	1.72	1.03
Eniwetok Beach Sand	1.33	E-8	1.72	0.69	34.5	33.1	1.72	1.72	1.03
Eniwetok Beach Sand	1.41	E-9	1.72	0.69	34.5	32.8	1.72	1.72	1.03
Eniwetok Beach Sand	1.45	E-10	1.72	0.69	34.5	33.1	1.72	1.72	1.03
Eniwetok Beach Sand	1.30	E-11*	1.72	0.69	34.5	32.9	1.72	1.72	1.03
Eniwetok Beach Sand	1.32	E-12	1.72	0.69	34.5	33.1	1.72	1.72	1.03
Eniwetok Beach Sand	1.32	E-13	1.72	0.69	-	-	1.72	1.72	1.03
Eniwetok Beach Sand	1.30	E-15	1.72	0.69	34.5	32.2	1.72	1.72	1.03

*0.13 mm brass shim stock used

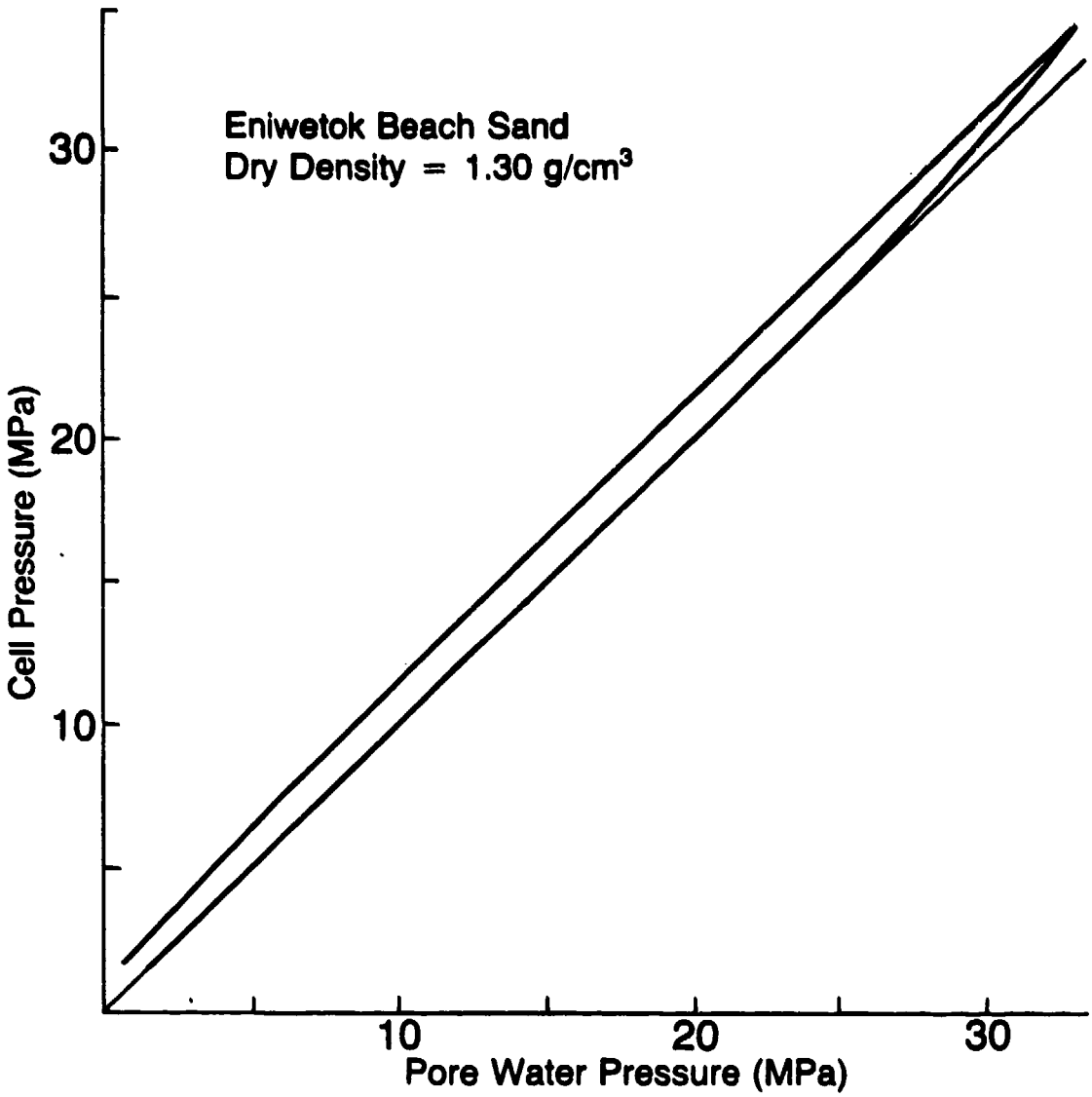

Fig. 9 Results of Test E-11

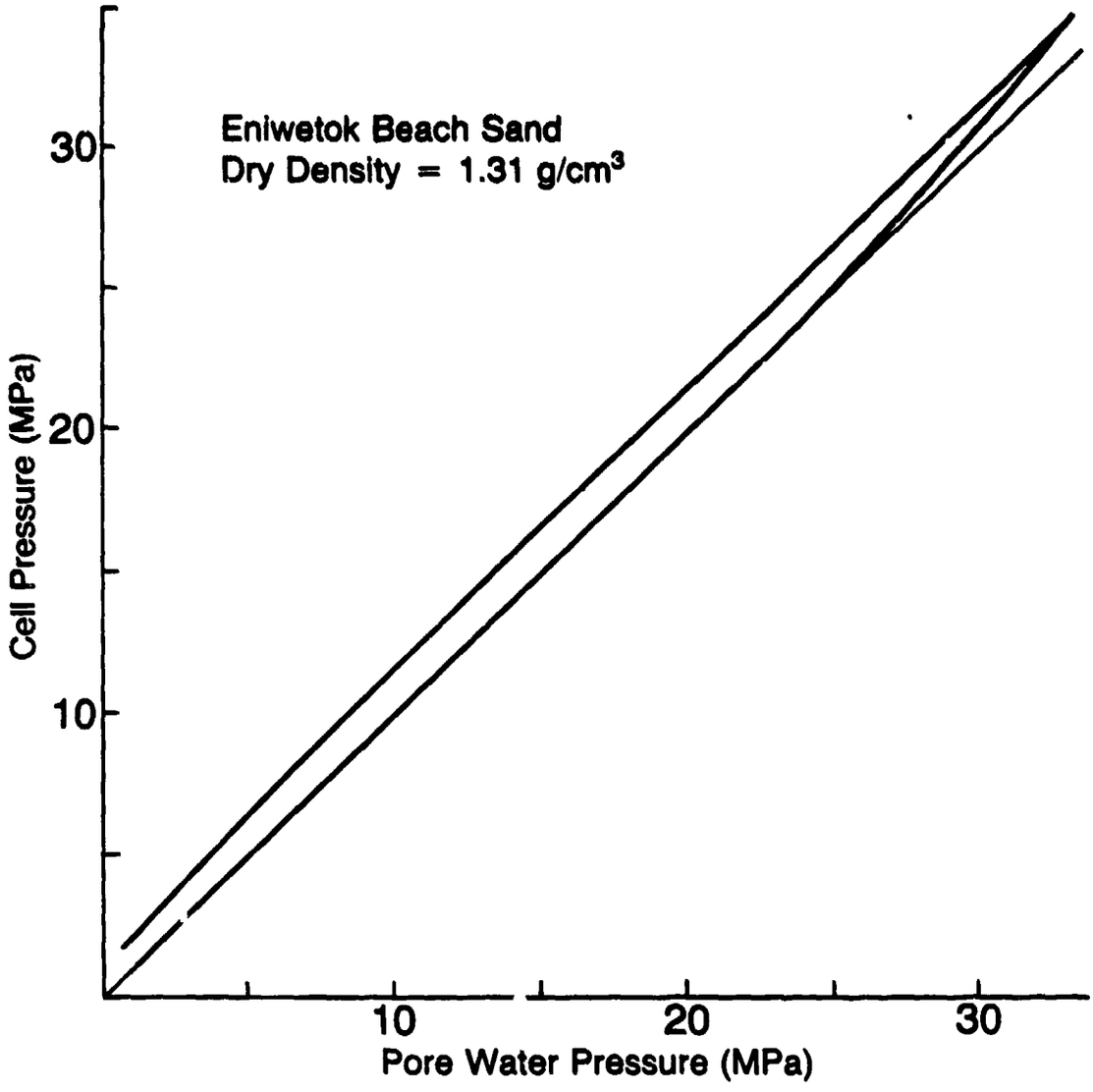

Fig. 10 Results of Test E-7

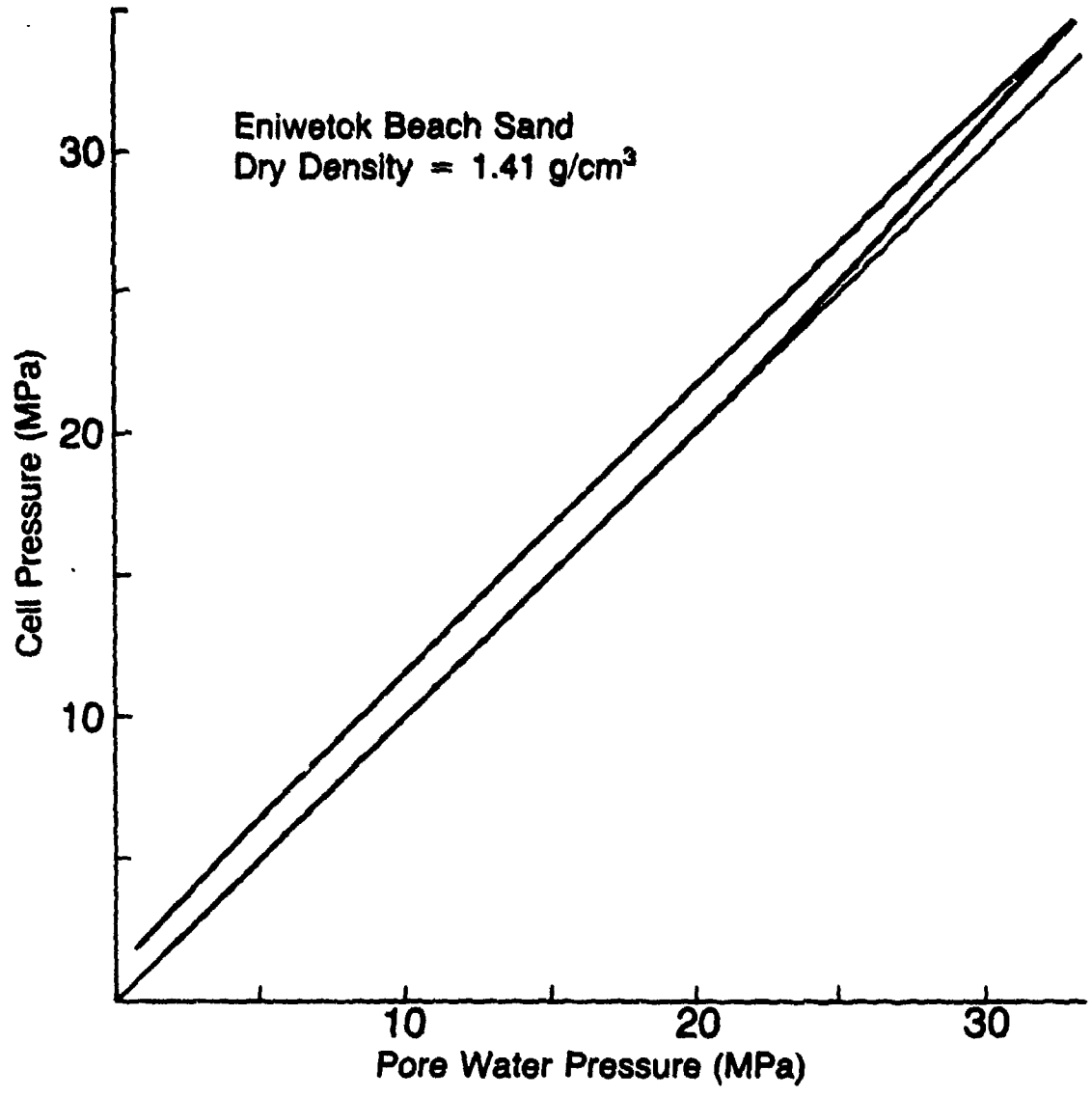

Fig. 11 Results of Test E-9

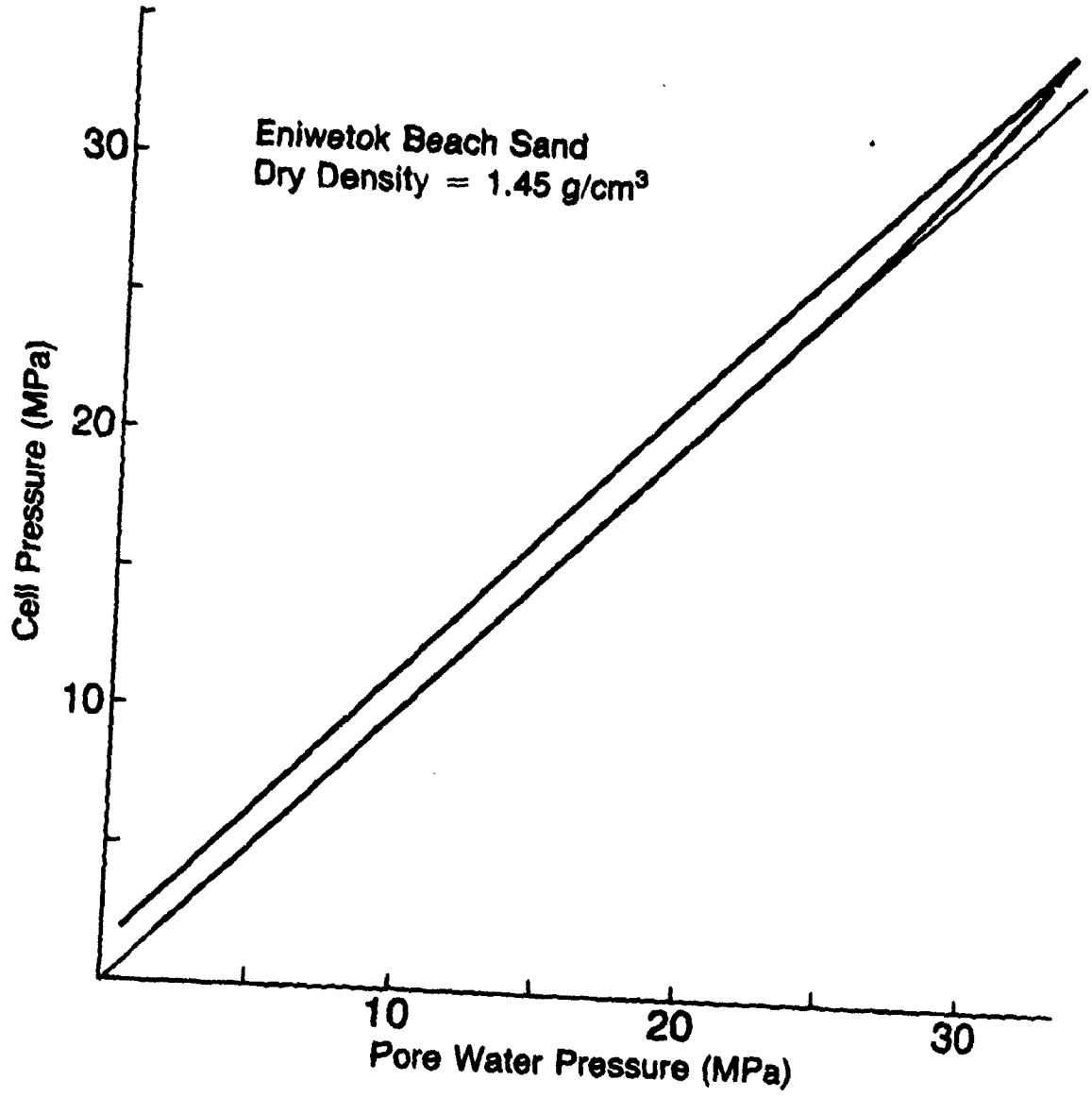

Fig. 12 Results of Test E-10

respectively. All the tests on Ottawa sands were conducted at or near minimum dry density.

The results of a test conducted on Flintshot sand are presented in Figure 13. The residual pore pressure observed at the end of this test was approximately 520 KPa, only one-half the pressure required to cause liquefaction. This test is similar to test E-7 in that subsequent to the initial cycle of loading the initial state of effective stress was reinstated and additional cycles were conducted. After each cycle the initial conditions were reimposed. Cycles to 6.9 and 13.8 MPa produced no observable residual pore pressure, but cycles to 20.7 and 27.6 MPa produced residual pore pressures of 172 KPa and 345 KPa, respectively.

The results of a test on a loose sample of Sawing sand are shown in Figure 14. These results closely match those obtained for Flintshot sand. The residual pore pressure observed was 520 KPa, one-half the initial effective stress.

The results of a third test, conducted on Banding sand, are shown in Figure 15. The residual pore pressure observed was 860 KPa, approximately 83% of that required to cause liquefaction. After the initial cycle the same series of cycles applied to the Flintshot sand was performed. The cycle to 6.9 MPa produced no measurable residual pore pressure, but the cycles to 13.8, 20.7 and 27.6 produced residual pore pressures of 170, 210 and 210 KPa, respectively.

The results of tests performed on Ottawa sands are presented in Table 4.

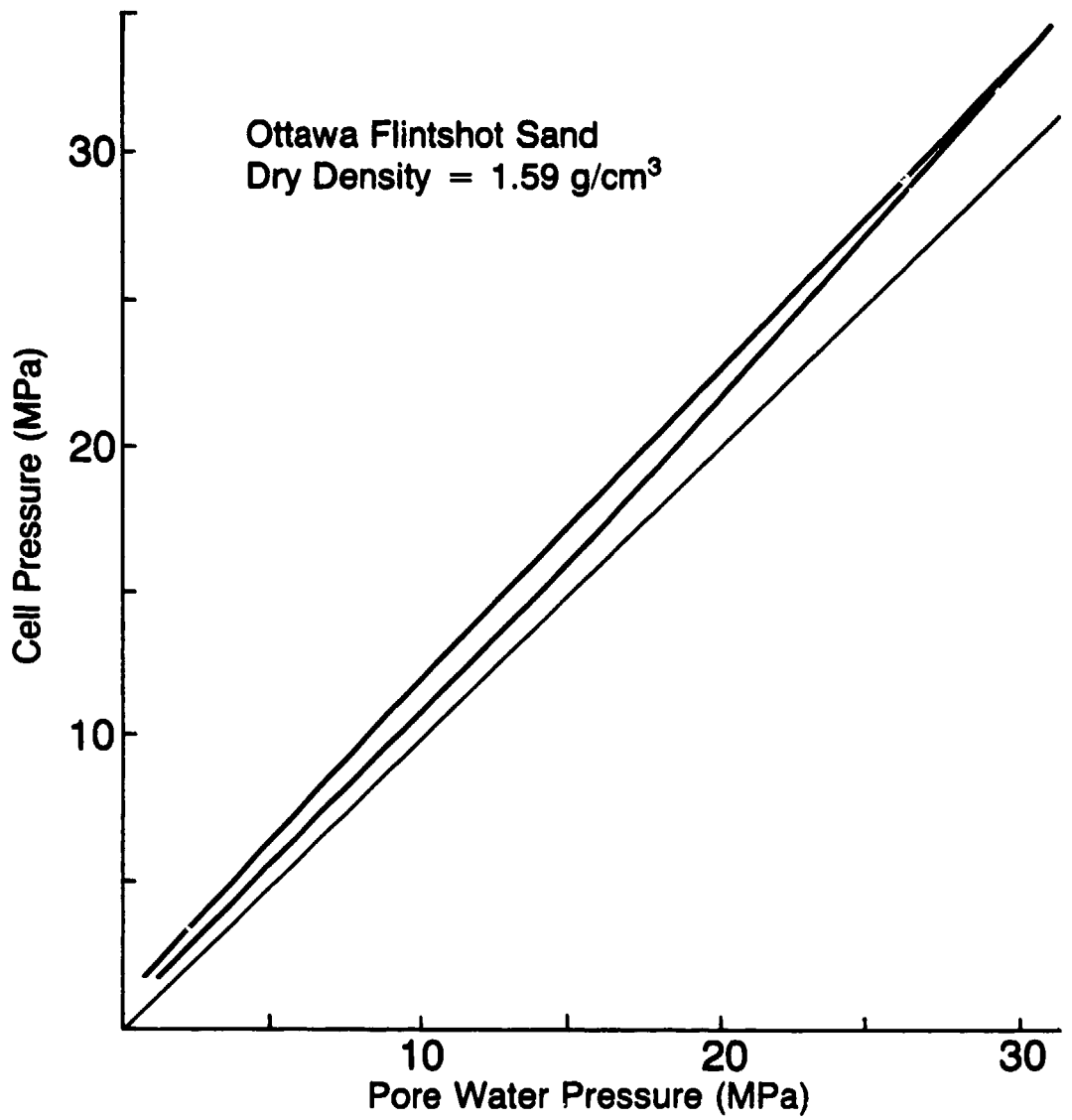

Fig. 13 Results of Test F-4

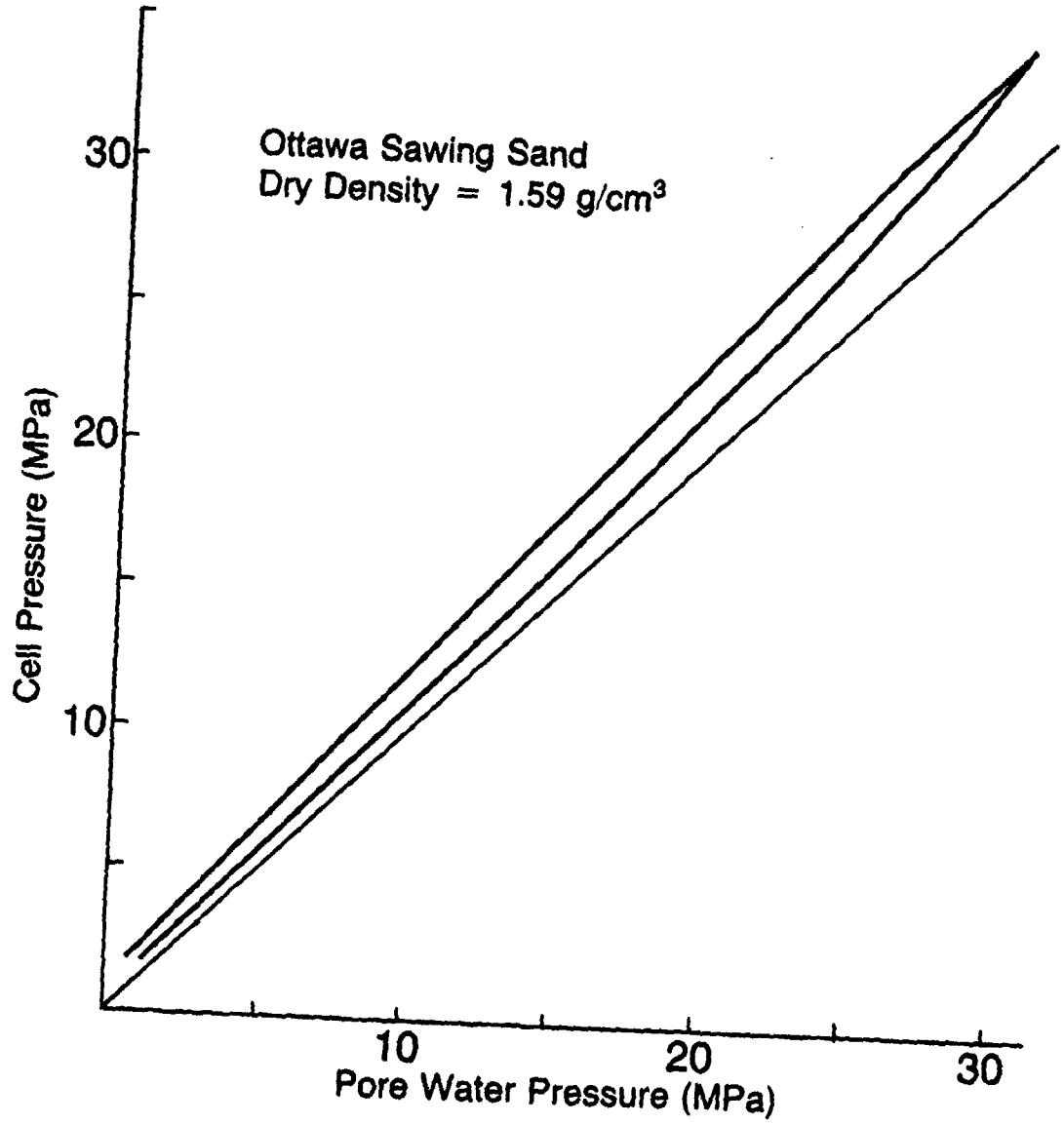

Fig. 14 Results of Test S-1

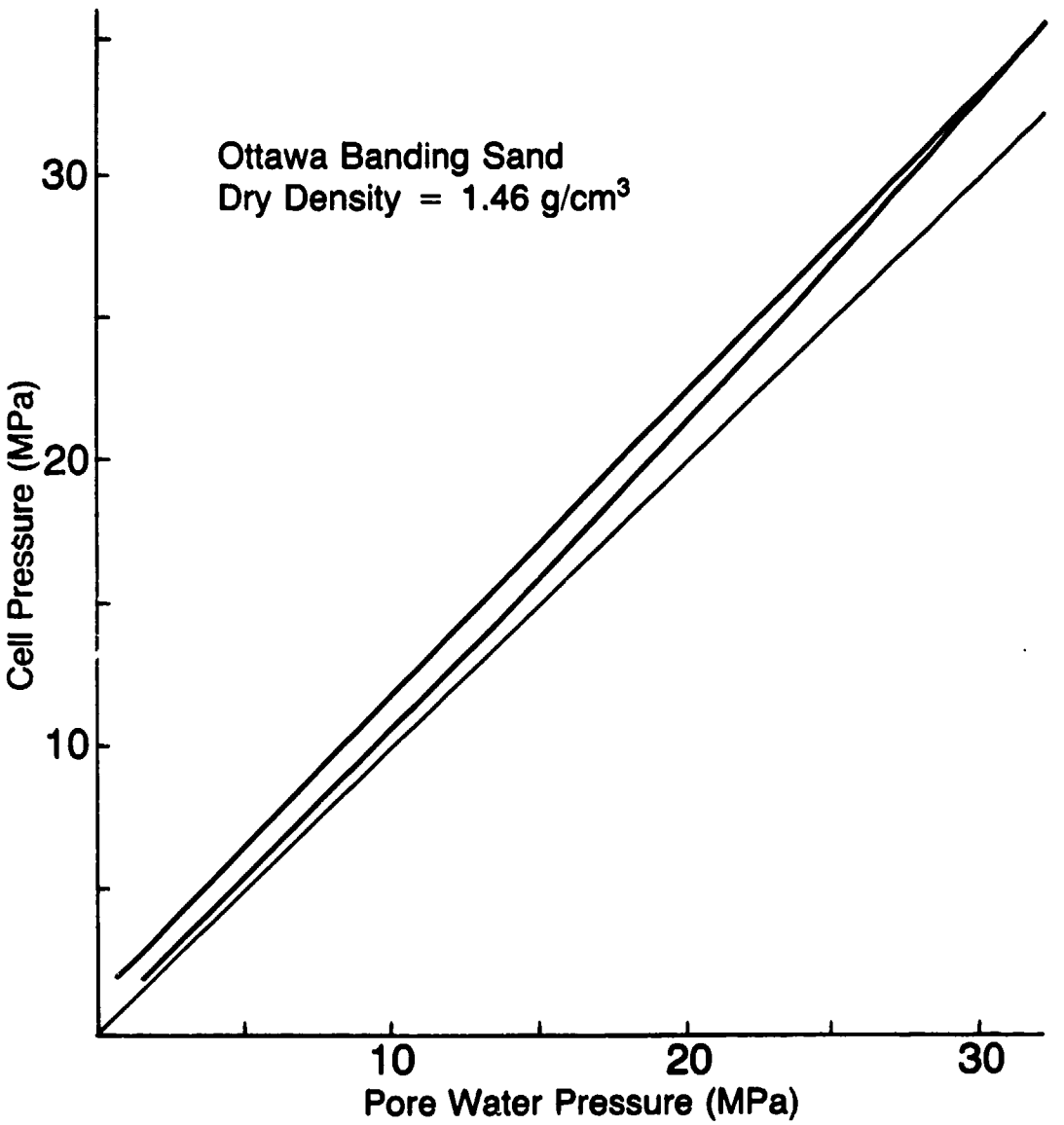

Fig. 15 Results of Test B-1

TABLE 4

Results of Tests on Ottawa Sand Conducted With Brass Shim Stock

Soil	Dry Density (g/cc)	Test	Initial		Peak		End		Residual Water Pressure (MPa)
			Confining Pressure (σ_3, MPa)	Water Pressure (u, MPa)	Confining Pressure (σ_3, MPa)	Water Pressure (u, MPa)	Confining Pressure (σ_3, MPa)	Water Pressure (u, MPa)	
Ottawa Flintshot	1.59	F-4	1.72	0.69	34.5	31.0	1.72	1.21	0.52
		"	1.72	0.69	6.90	5.34	1.72	0.69	0
		"	1.72	0.69	13.8	11.4	1.72	0.69	0
		"	1.72	0.69	20.7	17.6	1.72	0.86	0.17
		"	1.72	0.69	27.6	23.4	1.72	1.03	0.34
Ottawa Sawing	1.59	S-1	1.72	0.69	34.5	30.5	1.72	1.21	0.52
Ottawa Banding	1.46	B-1	1.72	0.69	34.5	31.4	1.72	1.55	0.86
		"	1.72	0.69	6.90	5.34	1.72	0.69	0
		"	1.72	0.69	13.8	11.5	1.72	0.86	0.17
		"	1.72	0.69	20.7	17.6	1.72	0.90	0.21
		"	1.72	0.69	27.6	24.1	1.72	0.90	0.21

SECTION V

DISCUSSION

5.1 INTRODUCTION

To properly model the proposed liquefaction mechanism it is necessary to perform completely undrained tests on samples which are 100% saturated. In this section the deviations from these conditions are discussed so that a proper interpretation of the test results can be made.

For reasons discussed below, we are confident that the tests were conducted on samples which were completely saturated. The deviations from "perfect" test conditions derive from drainage conditions. Truly undrained conditions are not present in the tests described above because of a) expansion of the steel tubing between the sample and the pore pressure transducer, b) deflection of the pore pressure transducer diaphragm, c) compression of the water in the tubing and valve between the sample and the pore pressure transducer, and d) membrane penetration.

The first three can be considered together as the compliance of the pore pressure measuring system. They have the effect of increasing the effective stress developed during the loading cycle and increasing the development of pore water pressure during unloading. Membrane penetration has the opposite effect. An analysis of the errors produced by these deviations from perfectly undrained conditions is presented below.

5.2 SAMPLE SATURATION

As mentioned above, past liquefaction experiments have been less than completely successful because the soil being tested was not 100% saturated. The carbon dioxide method of sample saturation, first described by Lade and Duncan (15), has been used successfully by the earthquake liquefaction researchers for several years, and produces 100% saturation when done properly (Houston, personal communication). As a check to determine if the time period allowed for sample saturation (overnight, with a minimum of 18 hours) was sufficient, a sample was prepared and allowed to saturate for 72 hours under a back pressure of .69 MPa. The results of this test were identical to a previous test in which only 18 hours were allowed for saturation.

Since the effect of partial saturation is to lower the susceptibility of a soil to liquefaction, and since liquefaction actually occurred in the Eniwetok tests, it was not felt that additional tests were required to prove that 100% saturation was accomplished.

5.3 EFFECTS OF COMPLIANCE OF THE PORE PRESSURE MEASURING SYSTEM

The flexibility of the pore pressure transducer, the tubing and valves connecting it to the sample, and the compressibility of the water in the measuring system all combine to allow water to flow out of the sample during the loading portion of the test. The effect of this alone is to produce a smaller change in pore water pressure in the sample during loading, and hence a larger effective stress compared to an inflexible system. Wissa (21) has expanded equation (2) to account for the effects of compliance of the pore pressure measuring system to:

$$B = \frac{1}{1 + n\frac{c_w}{m_v} + \frac{f_s}{V_o m_v}} \quad \ldots\ldots\ldots\ldots\ldots\ldots \quad (3)$$

in which V_o is the total volume of the sample and f_s is the total flexibility of the pore pressure measuring system. The flexibility of the system is measured in units of cubic centimeters per unit increase in pore water pressure. To calculate the flexibility for our test apparatus, the compression of water in the tubing and valves, the expansion of the tubing and the deflection of the transducer were calculated for a rise in water pressure of 34.5 MPa. The results of these calculations are a reduction in volume of water in the sample of 0.054, 0.0021, and 0.0002 cubic centimeters, respectively. This results in a calculated flexibility of 1.71×10^{-6} cc/KPa. Using the same maximum and minimum values for the volume compressibility of the soil skeleton and the above value of measuring system flexibility, the range of effects of flexibility on the pore pressure generated during loading can be determined. The calculated values of B are .9999 and .9508. The difference in generated pore pressure for an increase in cell pressure of 32.4 MPa is no more than 97 KPa, only 0.3% for a very stiff soil. There is virtually no difference for a very soft soil. During the unloading portion of the test the pore pressure will drop to almost exactly the same pressure as at the start of the test (within 3%). Since the response of the measuring system flexibility is small it will not significantly affect the results of the liquefaction test.

5.4 EFFECTS OF MEMBRANE PENETRATION

Penetration of the membrane enclosing the triaxial specimen into

the voids of the soil causes volume changes in tests where the effective confining pressure changes. The major difficulty in liquefaction tests comes when the effective stress in the sample is falling. This causes the membrane to move out from the soil voids, thereby increasing the volume of the sample. The pore pressure is, therefore, reduced compared to the magnitude it would have reached without membrane penetration. This phenomenon underestimates the susceptibility of a soil to liquefaction. The magnitude of the errors caused by membrane penetration is a function of the grain size, the void ratio of the soil, the changes in effective stress during the test and the surface area to volume ratio of the triaxial specimen. Lade (7) used brass shim stock plates between the triaxial membrane and the soil to reduce the effects of membrane penetration. He found that this reduced the effects by approximately 70% in his experiments. Frydman et al (18) have conducted tests to determine the effects of membrane penetration. They found that volume change due to membrane penetration increases linearly with the logarithm of effective stress. For this reason membrane penetration is most important at low effective stresses, when the soil is near liquefaction. On the basis of these tests, they developed a chart to estimate the volume change per unit surface area due to membrane penetration as a function of soil grain size and changes in effective stress. This chart was used to estimate the influence of membrane penetration in our tests. The volume change determined from the chart was reduced by two-thirds to account for the influence of the brass shim stock. For the loading portion of the test on Enfivetok sand the estimated flexibility due to membrane penetration is $.89 \times 10^{-5}$ cm^3 per KPa. This value is only correct

for an increase in effective stress from 0.69 MPa to 1.03 MPa. As the effective stress drops on unloading below .69 MPa the membrane flexibility will rise rapidly.

The combined effect of measuring system flexibility and membrane penetration can be determined by the following equation developed by Lade (7):

$$B = \frac{1}{1 + \frac{c_w}{m_v} + \frac{f_s}{V_o m_v} + \frac{f_m}{V_o m_v}} \quad \ldots\ldots\ldots\ldots\ldots\ldots \quad (4)$$

where f_m is the flexibility of the system due to membrane penetration.

Using the estimated flexibilities calculated above, a range in B values can be obtained for the combined effects of membrane penetration and measuring system compliance. For a soil skeleton compressibility of 2.04×10^{-3} m^2/KN the calculated B value is 0.9999. For a compressibility of 5.0×10^{-6} m^2/KN, the calculated B value is 0.9893. In both cases, the difference between the theoretical B value for a perfectly undrained test and for the B values which would be obtained with the predicted system compliance is negligible.

When the cell pressure is reduced during the unloading portion of the test, equation (4) can still be used to determine the change in water pressure as a function of change in cell pressure. The flexibility of the measuring system is the same during unloading as it is during loading, and the flexibility due to membrane penetration will be the same if the effective stress drops back to its original value (0.69 MPa). If the soil skeleton is elastic, then no residual pore pressure can be generated because the B value is the same as it was during loading. If, however, the soil skeleton becomes stiffer,

the value of B will decrease and, for the same change in cell pressure, will cause less change in water pressure. Ignoring the effects of membrane penetration, this means that when the cell pressure returns to its initial value of 1.7 MPa, the water pressure will be higher than 0.69 MPa, its original value. Liquefaction will occur if the difference in loading and unloading moduli is large enough.

Since the effects of membrane penetration increase rapidly as the effective stress nears zero, the actual generation of residual pore pressure will be less than would occur under undrained conditions. The fact that the Eniwetok sand did actually liquefy can, therefore, be taken as proof that the proposed mechanism can explain blast-induced liquefaction.

SECTION VI

FUTUPE WORK

6.1 ADDITIONAL QUASI-STATIC TESTS

The experiments described in this report have qualitatively demonstrated the validity of the blast-induced liquefaction mechanism. The ultimate goal of this line of research is to quantitatively describe the behavior of saturated, granular material and to use this information to predict the occurrence and effects of blast-induced liquefaction. Appropriate parameters are needed for a constitutive model so that this phenomenon can be numerically modeled.

The first experiments required to accomplish this goal should include precise testing of the specific effects of membrane penetration on Eniwetok sand and perhaps the Ottawa sands. The necessary equipment to do these tests has recently been obtained, and these tests are currently being performed. With the information necessary to very accurately calculate the membrane penetration term in Eq. (4), it will be possible to back calculate the soil compressibility (both loading and unloading) from the results of an undrained test. Tests should then be performed to determine the soil compressibility from drained tests over the same range of effective stress. If the volumetric behavior of sand is truly governed by effective stress alone, the two methods of calculating volume compressibility should give the

same results. It is important to determine if they are the same, since it is easier to run drained compression tests to measure compressibility than to run the type of undrained test described in this report.

After the information described above has been obtained, it will be important to do a series of parametric studies to determine the influence of various soil parameters on the liquefaction susceptibility of Eniwetok and other sands. These tests should be designed to determine the influence of initial void ratio (density), initial stress state, grain size and distribution, and particle shape on liquefaction susceptibility.

After the tests described above have been completed, it should be possible to describe mathematically the behavior of a saturated sand during undrained isotropic loading. Attention should then be turned to a more accurate description of the true loading cycle caused by an explosion. Anisotropic loading conditions should be modeled with a more sophisticated testing setup. It is likely that computer controlled loading would be necessary. These tests would be considerably more difficult to conduct and to interpret, and it is not necessarily true that the added information would be important enough to warrant the data collection. For these reasons, it is felt that the isotropic loading case should be investigated thoroughly before attempts are made to conduct anisotropic tests.

6.2 OTHER MODEL TESTS

All the tests proposed above have one problem in common--they are all quasi-static tests. At some point in the research effort, it will be necessary to conduct dynamic experiments. There are at least four different ways in which dynamic experiments could be conducted.

The existing testing apparatus could be modified so that the cell pressure is increased dynamically. A miniaturized pore pressure transducer would have to be placed in the specimen and the oil pressure would have to be measured in the cell. The mechanics of such a modification might be difficult and expensive, especially since the authors know of no such system in existence. Experiments using the modified equipment would determine if the volumetric behavior of Eniwetok and other sands is significantly different under dynamic loading conditions. No information would be obtained on the behavior of a large deposit of soil or on the effects of partial drainage on the blast-induced liquefaction mechanism. To model deposits of sand the following three test methods may be more appropriate.

A second alternative would be to conduct shock tube experiments. It should be possible to saturate a container of soil in much the same way as was done in the experiments described above. This method has been used successfully to saturate a large container of sand for shake table tests (Seed, personal communication). Miniature pressure transducers would have to be placed in the soil to obtain qualitative results, but this should not present any difficulty. The major drawback to shock tube experiments is that it is not possible to model the initial stress distribution in a deep deposit of soil. Since the compressibility of sand is a function of confining pressure, it is likely that the initial stress distribution will play an important role in the behavior of a real deposit of sand.

The third alternative is to do small scale laboratory cratering experiments. Again, the CO_2 method of saturation could be used in a large bin of soil. This method suffers from the same problem as the

previous method. It is not possible to model the initial state of stress in the soil.

The last method is to conduct cratering experiments in a centrifuge. The problem of saturation in the model bucket is no different than with non-centrifuge tests. The initial stress distribution of the soil deposit can be matched almost exactly in the centrifuge model. This is very important for cratering experiments, as Schmidt and Holsapple (22, 23) have shown from a similarity analysis for the thermomechanical response of a continuum that increased gravity is a necessary condition for subscale testing when identical material for both model and prototype is used. The cubic scaling on yield in centrifuge experiments also makes it very attractive for modeling high yield explosions (kiloton and up).

SECTION VII

SUMMARY AND CONCLUSIONS

A series of high pressure undrained isotropic compression tests have been performed on Eniwetok Beach sand and three types of Ottawa sand--Flintshot, Banding and Sawing. The objective was to verify a mechanism which has been proposed to explain blast-induced liquefaction. The central assumption of this theory is that the sand skeleton will undergo plastic volume change during a cycle of undrained loading. The tests consisted of first saturating cylindrical samples of sand in a high pressure triaxial cell with a cell pressure of 1.72 MPa and a pore water pressure of 0.69 MPa. After saturation, the cell pressure was increased to 34.5 MPa, then reduced to 1.72 MPa. During this cycle the pore water pressure was measured and plotted vs. cell pressure on an X-Y recorder. The pore water pressure was found to be larger at the end of the cycle than at the beginning. In the tests on Eniwetok sand this difference was sufficient to cause liquefaction. An analysis of the errors caused by deviations from true undrained loading was also performed. It was shown that for the purpose of verifying the blast-induced liquefaction mechanism, these errors were not significant.

On the basis of these findings, the following conclusions can be reached:

1. The blast-induced liquefaction mechanism proposed by Prater (4) and Rischbieter et al (5) has been verified for quasi-static, isotropic loading.
2. Eniwetok beach sand is considerably more susceptible to blast-induced liquefaction compared to Ottawa sand.
3. The stress required to cause liquefaction in Eniwetok sand is well within the range of compressive stresses produced by high energy and thermonuclear explosions.
4. Additional laboratory tests are required to quantify the volumetric behavior of sands, especially Eniwetok sand, to provide the necessary information for numerical modelers.
5. Dynamic tests are required to investigate the effects of the very small rise time for the compression wave in the field, and the effects of partial drainage. Centrifuge model tests have been suggested as the best way, short of full scale field testing, to investigate these topics.

APPENDICES

APPENDIX A: REFERENCES

APPENDIX B: SYMBOLS

REFERENCES

1. Committee on Soil Dynamics of the Geotechnical Engineering Division, ASCE, "Definition of Terms Related to Liquefaction," Journal of the Geotechnical Engineering Division, ASCE, Vol. 104, No. GT9, Sept., 1978.

2. Melzer, L. S., "Blast-Induced Liquefaction of Materials," AFWL-TR-78-110, Air Force Weapons Laboratory, Kirtland Air Force Base, NM, 1978.

3. Blouin, Scott E., "Blast-Induced Liquefaction," Civil Systems, Incorporated Report CSI IR 79-001 (draft), 1979. To be published as an Air Force Weapons Laboratory Report.

4. Prater, E. G., "Pressure Wave Propagation in a Saturated Soil Layer with Special Reference to Soil Liquefaction," Proc. Fifth Intl. Symposium on Military Applications of Blast Simulation, Vol. II, Royal Swedish Fortifications Admin., Stockholm, Sweden, May, 1977, pp. 7:3:1-7:3:23.

5. Rischbieter, F., Cowin, P., Metz, K. and Schapermeier, E., "Studies of Soil Liquefaction by Shock Wave Loading," Proc. Fifth Intl. Symposium on Military Applications of Blast Simulation, Vol. III, Royal Swedish Fortifications Admin., Stockholm, Sweden, May, 1977.

6. Skempton, A. W., "The Pore Pressure Coefficients A and B," Geotechnique, London, England, Vol. 4, No. 4, 1954, pp. 143-147.

7. Lade, Poul V. and Hernandez, Sonia B., "Membrane Penetration Effects in Undrained Tests," Journal of the Geotechnical Engineering Division, ASCE, Vol. 103, No. GT12, Proc. Paper 12758, Feb., 1977, pp. 109-125.

8. Ishihara, K., "Propagation of Compressional Waves in a Saturated Soil," Proceedings, Intl. Symposium on Wave Propagation and Dynamic Properties of Soils, Albuquerque, NM, Aug., 1977, pp. 451-467.

9. Lyakhov, G. M., and Polyakova, N. I., Waves in Solid Media and Loads on Structures, FTD-MT-24-1137-71, Defense Documentation Center, Alexandria, VA, March, 1972, from Volny v Plotnykh Sredakhi Nagruzki na Sooruzheniya, 1967.

10. Cristescu, N., Dynamic Plasticity, North-Holland Publishing Co., Amsterdam, 1967, p. 515.

11. Kok, L., "The Effect of Blasting in Water Saturated Sands," Proc. Fifth Intl. Symposium on Military Applications of Blast Simulation, Vol. II, Royal Swedish Fortifications Admin., Stockholm, Sweden, 1977.

12. Studer, J., and Hunziker, E., "Experimental Investigation on Liquefaction of Saturated Sand Under Shock Loading," Proc. Fifth Intl. Symposium on Military Applications of Blast Simulation, Royal Swedish Fortifications Admin., Stockholm, Sweden, May, 1977.

13. Richart, F. E., Hall, J. R., and Woods, R. D., Vibrations of Soils and Foundations, Prentice-Hall, Inc., Englewood Cliffs, NJ 1970.

14. Rischbieter, F., "Soil Liquefaction--a Survey of Research," Proc. Fifth Intl. Symposium on Military Applications of Blast Simulation, Vol. III, Royal Swedish Fortifications Admin., Stockholm, Sweden, May, 1977.

15. Lade, P. V., and Duncan, J. M., "Cubical Triaxial Tests on Cohesionless Soil," Journal of the Soil Mechanics and Foundations Division, ASCE, Vol. 99, No. SM10, Proc. Paper 10057, October, 1973, pp. 793-812.

16. Black, David K., and Lee, Kenneth L., "Saturating Laboratory Samples by Back Pressure," Journal of the Soil Mechanics and Foundation Engineering Division, ASCE, Vol. 99, No. SM2, Jan., 1973, pp. 75-93.

17. Windham, J. E., "Material Property Investigation for Project Micro Atoll: Subsurface Exploration and Laboratory Test Results," Interim Report, April, 1973 (draft prepared for AFWL).

18. Frydman, S., Zeitlen, J. G., and Alpan, I., "The Membrane Effect in Triaxial Testing of Granular Soils," Journal of Testing and Evaluation, Vol. 1, No. 1, Jan., 1973, pp. 37-41.

19. Martin, Geoffrey R., Finn, W. D. Liam, and Seed, H. Bolton, Effects of System Compliance on Liquefaction Tests," Journal of the Geotechnical Engineering Division, ASCE, Vol. 104, No. GT4, Proc. Paper 13667, April, 1978, pp. 463-479.

20. Raju, V. S., and Sadasiuan, S. K., "Membrane Penetration in Triaxial Tests on Sands," Journal of the Geotechnical Engineering Division, ASCE, Vol. 100, No. GT4, Proc. Paper 10454, April, 1974, pp. 482-489.

21. Wissa, A. E. Z., "Pore Pressure Measurement in Saturated Stiff Soils," Journal of the Soil Mechanics and Foundations Division, ASCE, Vol. 95, No. SM4, Proc. Paper 6670, July, 1969, pp. 1063-1073.

22. Schmidt, R. M., and Holsapple, K. A., "Theory and Experiments on Centrifuge Cratering," J. Geophys. Res., Vol. 84, No. B13, 1979.

23. Schmidt, R. M., and Holsapple, K. A., "Centrifuge Crater Scaling Experiments I: Dry Granular Soils," Defense Nuclear Agency Report DNA 4568F, Washington, DC, 177 pp., 1978.

SYMBOLS

B	pore pressure parameter
V_o	initial volume
c_w	compressibility of water
f_m	flexibility due to membrane penetration
f_s	flexibility due to pore pressure measuring system
m_v	compressibility of soil matrix
n	porosity
u	pore water pressure
Δu	change in pore water pressure
σ_3	confining (cell pressure)
$\Delta\sigma_3$	change in confining (cell) pressure